Muscle Cs-137 in Fukushima wildlife from rescue and wildlife-control programmes

Hisashi Komatsu[a,b,*], Kiemi Murakami[a], Kousuke Kanda[a], Masahiko Kabeya[c], Kenji Inami[c]

[a] Fukushima Prefectural Centre for Environmental Creation, 10-2 Fukasaku, Miharu, Fukushima, 963-7700, Japan
[b] Fukushima Regional Collaborative Research Center, National Institute for Environmental Studies, 10-2 Fukasaku, Miharu, Fukushima, 963-7700, Japan
[c] Fukushima Wildlife Symbiosis Center, 67 Nagakubo, Tamai, Ootama Village, Fukushima, 969-1302, Japan

* Corresponding author: Hisashi Komatsu, Fukushima Regional Collaborative Research Center, National Institute for Environmental Studies, 10-2 Fukasaku, Miharu, Fukushima, 963-7700, Japan. E-mail: hisashikomatsu2015@gmail.com

Abstract

We analysed opportunistic muscle Cs-137 records of wild mammals and birds from rescue and wildlife-control programmes in Fukushima Prefecture, Japan, in 2017–2025. Bayesian hierarchical models, with species random intercepts and left-censored non-detects, related concentrations to a fixed baseline contamination index, the 2012 air dose rate at capture locations. In 182 records of 38 species, a 10-fold higher index was associated with 13.8-fold higher concentrations, adjusted for year and species (95% credible interval [CrI] 8.80–22.1). The ratio was 13.7 (7.55–25.2) with a municipality random intercept and 12.9 within species. Species differed widely (species SD 1.21, 95% CrI 0.80–1.79, a 3.35-fold difference), mostly between classes. With class as a fixed effect, mammals exceeded birds 8.70-fold (95% CrI 4.88–16.6) and the species SD fell to 0.47. Temporal estimates were not robust in direction across specifications and were indistinguishable from physical decay. Because later years had more mammal records (3 of 43 from 2024 were birds) and the year effect was positive between species but negative within species, pooled year estimates partly reflect changing species composition. In two planned guild contrasts with aquatic-associated birds, muscle Cs-137 was 10.3-fold higher in soil/litter-associated mammals (95% CrI 4.80–23.4), whereas other terrestrial birds did not differ clearly (ratio 1.56, 0.716–3.47). The two mammal guilds did not differ clearly (ratio 0.869, 0.291–2.34); a class-only model fitted equally well. Guilds that included class thus largely reproduced the mammal–bird difference, which may also reflect unrecorded time in care or foraging range. Multispecies radiocaesium data should be analysed with species-level effects.

Keywords

Radiocaesium; Fukushima Daiichi nuclear accident; Wildlife; Hierarchical Bayesian model; Left-censored data; Air dose rate

1. Introduction

The March 2011 Fukushima Daiichi Nuclear Power Plant accident deposited 2.7 PBq of Cs-137 on land, 67% of it on forests, where it remains near the soil surface (Onda et al., 2020). Game mammals and birds have been monitored across Fukushima Prefecture since 2011 (Fukushima Prefecture, 2026). Exceedances of the radiocaesium food standard in wild meat have declined but still occur (Ministry of the Environment, 2026). An international assessment reported high radiocaesium levels and transfer in several game species, with an initial rapid decline followed by slower decreases (UNSCEAR, 2022). Because wild animals integrate contamination from their habitats and food webs, they are useful indicators of this persistent contamination.

In Fukushima, muscle Cs-137 in wild mammals has often been positively associated with contamination at the capture site, measured from deposition maps or soil categories. Examples include Asian black bear (*Ursus thibetanus*) and wild boar (*Sus scrofa*; Nemoto et al., 2018) and Japanese monkeys (*Macaca fuscata*; Hayama et al., 2013). These associations were not observed in every landscape (Anderson et al., 2019; Saito et al., 2022a). Temporal trajectories also vary: transfer from soil declined in some game species but showed no clear trend in others (Tagami et al., 2016). In wild boar, concentrations declined at region-specific rates over 14 years of monitoring (Komatsu and Ikushima, 2026). A pooled temporal trend may therefore describe multispecies data poorly, because it can depend on which species are sampled and when. Temporal slopes can also be compared with the decline expected from the physical decay of Cs-137 alone.

Co-occurring species can differ widely in muscle Cs-137 and in transfer from soil (Tagami et al., 2016; Watanabe et al., 2014). In eastern Nihonmatsu, for example, four mammals had higher muscle Cs-137 than three birds from the same area, although the samples were small (Watanabe et al., 2014). The mammals were wild boar, masked palm civet (*Paguma larvata*), raccoon dog (*Nyctereutes procyonoides*) and badger (*Meles anakuma*), and the birds were carrion crow (*Corvus corone*), green pheasant (*Phasianus versicolor*) and spot-billed duck (*Anas zonorhyncha*). Foraging ecology and trophic position are often proposed as explanations for such differences. In one forest, Cs-137 was concentrated in litter and moved to invertebrate consumers mainly through the detrital food chain (Murakami et al., 2014). In one catchment, forest food webs carried more Cs-137 than stream food webs (Sakai et al., 2016). Aquatic-associated species do not consistently have low concentrations, however (Saito et al., 2022b; Stocki and Braune, 2020). The existing evidence therefore does not support a general ranking of terrestrial above aquatic species.

Many wildlife analyses in Fukushima have focused on one or two hunted or culled game species (Nemoto et al., 2018) or have summarised transfer by species from aggregated monitoring data (Tagami et al., 2016). Comparisons of sympatric mammals and birds remain few and small (Watanabe et al., 2014). Mixed models that separate species from site effects have been applied to other radioecological data, such as fish (Beresford et al., 2013). Few analyses of wild mammals and birds have jointly considered contamination, time and differences among species. Where trait-based groups, such as terrestrial and aquatic feeders, also differ in taxonomic class, their differences are difficult to distinguish from those between mammals and birds. It

therefore remains unclear whether ecological groups defined from traits capture differences beyond those between taxonomic classes.

Here we analysed muscle Cs-137 in wild mammals and birds from rescue and wildlife-control programmes in Fukushima Prefecture. The main analyses used dried samples from animals captured in 2017–2025. The records come from these programmes, not from hunting, and therefore include non-game species such as raptors and herons. Because they cover many species and were all measured in one laboratory, they allow the size of species differences, and their effect on pooled estimates, to be quantified. Using hierarchical models with species random intercepts and left-censored non-detects, we addressed four questions. (i) Is muscle Cs-137 associated with a fixed baseline environmental contamination index (the 2012 air dose rate at the capture location, from the fifth airborne monitoring survey), and does the association hold within species? (ii) How is muscle Cs-137 associated with time since the accident, how does the temporal slope compare with physical decay, and do pooled estimates of the temporal association reflect changes in species composition? (iii) How large is the heterogeneity among species? (iv) Do ecological guilds defined from species traits explain differences among species beyond those between taxonomic classes?

2. Materials and methods

2.1. Wildlife records and study design

We analysed muscle Cs-137 records of wild mammals and birds captured in Fukushima Prefecture, Japan, from 2013 to 2025. The records were compiled in a single master dataset, held by the Fukushima Prefectural Centre for Environmental Creation (the Centre). The records are opportunistic: they arise from rescue and wildlife-control activities, not from a sampling design. No animal was captured or euthanised for this study, and no live-animal experiment was conducted. Only muscle tissue collected post mortem was used. Injured or diseased animals rescued through prefectural programmes were handled by prefectural veterinarians and subsequently died. Raccoons (*Procyon lotor*) and masked palm civets were captured and euthanised with an electric lance under routine wildlife-control programmes, independently of the present research. The origin of each animal (rescue or control capture) was not recorded for individual records. Origin was therefore classified by species: raccoon and masked palm civet as control-captured (38 of the 182 records of the index model; Section 2.5) and all other species as rescued.

The 11 wild boar (*Sus scrofa*) records in the master dataset were excluded before all analyses. Wild boar is a target species of the prefecture's routine monitoring for shipping restrictions on game meat (Fukushima Prefecture, 2026; Komatsu and Ikushima, 2026), and the source of the wild boar records in the master dataset (rescue or another programme) could not be confirmed. Of these records, 2 met the inclusion criteria of the main analyses.

Ten raptor measurements, from individuals rescued in 2013–2015, are the same measurements of the same individuals that were reported previously (Saito et al., 2019) and do not provide independent replication of

that study. They entered only the secondary analyses that span both measurement periods (fresh and dried samples; Section 2.6), not the main analyses of dried samples or the guild analyses.

2.2. Radiocaesium measurements

All Cs-137 measurements were made at the Centre by gamma-ray spectrometry with germanium semiconductor detectors. This method was used throughout the study period, although sample preparation changed from fresh to dried samples (below), and sample masses and counting times varied. Detector-level settings and the parameters used to calculate limits of detection (LODs) were not stored with individual records. Concentrations and LODs were therefore used as reported by the Centre. Carcasses were kept frozen from the sampling date (the date of capture or, for rescued animals, of death) until processing, and the Centre reported activity concentrations decay-corrected to that date. Samples were measured fresh for animals captured in 2013–2017. Samples from animals captured in 2017–2025 were measured after drying, in measurement campaigns in 2022, 2024 and 2025. The last fresh-sample capture and the first dried-sample capture were both on 5 September 2017. Activity concentrations and LODs of dried samples were converted to a wet-weight basis using the dry-matter fraction of each sample. Only Cs-137 was analysed, because Cs-134 was detected in only 14 or 15 of the 182 index-model samples (Section 2.5), depending on the gamma line used.

2.3. Measurement status and data processing

Each Cs-137 result was classified from the recorded values as detected, a non-detect with a recorded LOD, a non-detect without a usable LOD or not measured. Numerical values reported below the LOD were treated as non-detects at that LOD, and missing LODs were not imputed. In the censored concentration models, non-detects with a recorded LOD were represented as left-censored observations at their LODs (Helsel, 2006). In the detection models, they were coded as not detected. Non-detects without a usable LOD (26 records, all from fresh samples) could not be censored at a threshold. They were used only as non-detects in the secondary detection models. One non-detect was excluded because its recorded wet-weight LOD (23,577 Bq/kg) exceeded the highest detected concentration in the population (9,593 Bq/kg). As a left-censored value, it would carry almost no information, and including it changed the estimates little (Section 3.6). All data processing was scripted and documented. Species names recorded in Japanese were mapped to the GBIF Backbone Taxonomy (GBIF Secretariat, 2023), and bird names were checked against the Check-list of Japanese Birds (Ornithological Society of Japan, 2024).

2.4. Fixed baseline environmental contamination index

The environmental predictor was the air dose rate at 1 m above the ground (μSv/h, including natural radionuclides) from the fifth airborne monitoring survey, decay-corrected to 28 June 2012 (MEXT, 2012). This survey was chosen because it covers the whole prefecture on a single standard mesh and represents the early, post-deposition baseline of contamination before most decontamination. Each capture location was assigned the index of its quarter-grid square (JIS X 0410) by exact code match, without spatial imputation.

Values recorded only as below 0.1 μSv/h (left-censored) were not converted to numbers, and these 3 records were excluded from the models that used the index. A bounding sensitivity analysis is described in Section 2.8. The index was $\log_{10}$-transformed. It serves as a fixed baseline spatial index of the early contamination gradient at the capture location and is not a measure of individual exposure.

2.5. Analysis populations

Main analyses used measurements of dried samples only, because a single temporal slope across both measurement periods would have been confounded with the change in measurement basis. The analysed captures therefore spanned 5 September 2017 to 14 June 2025. Records also required a capture date recorded to the day, a uniquely identified species and no data-quality flag on the Cs-137 result. The two species-adjusted models (Section 2.6) used different populations. The species-adjusted index model required an assigned, uncensored index value but not a recorded region. It used 182 records of 38 species (50 left-censored), with index values of 0.1 to 13 μSv/h. The species-adjusted regional model instead required a recorded administrative region of capture (Aizu, Nakadori or Hamadori). It used 226 records of 39 species, of which 59 were left-censored. Neither population contains the other. Of the regional population, 45 records had no index value: 41 lacked valid coordinates (31 of them captured in 2024), 3 had a censored index and 1 had a data-quality flag on its coordinates. Conversely, one record of the index population had no recorded region. The guild model used the full index population (Section 2.7). The observational unit was the muscle record of one animal. In the main models, records were treated as independent given species, and clustering by capture event and by municipality was examined in sensitivity analyses (Section 2.8). Three records sharing one individual identifier could not be confirmed as distinct individuals; they were retained as separate records and belong to one capture event.

2.6. Statistical models

The three main models were the species-adjusted index model, the species-adjusted regional model and the guild model (Section 2.7). All three were Bayesian Gaussian regressions of natural-log wet-weight muscle Cs-137 concentration, with non-detects that had a recorded LOD left-censored at their log wet-weight LOD. Time since the accident (hereafter 'year'), from 11 March 2011 to the capture date, was expressed in years as elapsed days divided by 365.25. The species-adjusted index model included year, the $\log_{10}$ index and a random intercept for species. The species-adjusted regional model replaced the index with a fixed effect of region, with Nakadori as the reference. Because it did not require coordinates, it also used records without an index value. Year and index effects were common to all species, and species-specific slopes were not fitted. To examine whether the associations held within species, a version of the species-adjusted index model split year and the $\log_{10}$ index each into two components. The between-species component was the species mean, and the within-species component was the deviation of each record from its species mean. Companion models had the same predictors as the species-adjusted models but no species term, and they show how the year and index estimates change when between-species heterogeneity is modelled. They were fitted both to

their own populations, which also include records without a unique species identification, and to the same records as the species-adjusted models.

Secondary models were of two kinds. Logistic detection models and Gaussian models of detected concentrations spanned both measurement periods, each with a measurement-period term. A logistic detection model of the index-model population included the log LOD and the $\log_{10}$ index. All secondary models included year and a species random intercept.

2.7. Ecological traits and guild models

Four core traits (taxonomic class, broad diet, soil/litter contact and dependence on aquatic food webs) were coded for each species by fixed rules, without reference to Cs-137 data. Broad diet was derived from the diet percentages in EltonTraits 1.0 (Wilman et al., 2014), and documented qualitative evidence from Japan could override the database category. For carrion crow and large-billed crow (*Corvus macrorhynchos*), the override changed the broad diet, and the species were therefore assigned to G5 instead of G4, the guild implied by the database category (guilds are defined below). Soil/litter contact was coded primarily from the foraging-stratum information in EltonTraits 1.0 (Wilman et al., 2014). Aquatic dependence (obligate, facultative or none) was coded from the predominance or documented repeated use of aquatic food, using AVONET trophic niches for birds (Tobias et al., 2022). Habitat or life on the water surface alone did not determine dependence. Guilds were then derived from the four traits by an ordered rule table, without using Cs-137 measurements, index values or model results. The two mammal guilds were G1, soil/litter-associated terrestrial mammals (82 records, 6 species), and G2, terrestrial herbivorous mammals with low or medium soil/litter contact (9 records, 4 species). G1 comprised omnivorous or animal-eating mammals with high or medium soil/litter contact. The three bird guilds were G3, aquatic-associated birds (33 records, 11 species); G4, terrestrial vertebrate-eating birds (24 records, 5 species); and G5, other terrestrial birds, that is, herbivorous, omnivorous or invertebrate-eating species (31 records, 11 species). American mink (*Mustela vison*; 3 records), the only mammal coded as using aquatic food, formed a residual group. Guild labels summarise the coded traits. Because taxonomic class is one of the traits, every guild lies within one class: G1 and G2 are mammals, and G3, G4 and G5 are birds.

The guild model added a guild fixed effect to the species-adjusted index model. It kept the common year and index slopes and the species random intercept and had no guild interaction with the index or year. The five guilds and the residual group entered one model, and all contrasts between them were computed from the same posterior, with aquatic-associated birds (G3) as the reference category. G1 − G3 and G5 − G3 were the planned contrasts, specified before any guild model was fitted. The other contrasts, including G1 − G2, were exploratory. G1 − G3 and G5 − G3 were also estimated in a guild model of the G1, G3 and G5 records, and G4 − G3 in a model of the G3 and G4 records. These subset guild models do not include masked palm civet or Eurasian coot. Between-species heterogeneity with and without the guild term was compared using the species standard deviation (SD) estimated by the species-adjusted index model and by the guild model, both fitted to the same records. To examine whether the guilds captured differences beyond those between classes,

a class-only model replaced the guild term by taxonomic class (mammal or bird) and was compared with the guild model by Pareto-smoothed importance-sampling leave-one-out cross-validation (PSIS-LOO), computed with brms.

Question (i) was addressed by the index coefficient of the species-adjusted index model and its within-species component. Question (ii) was addressed by the year coefficients, their comparison with physical decay (Section 2.9) and the within- and between-species components of year. Question (iii) was addressed by the species SD, and question (iv) by the guild model and its comparison with the class-only model.

2.8. Sensitivity analyses

Each sensitivity analysis changed one assumption of a main model. One population check added back the record excluded for its LOD (Section 2.3). Others excluded, one at a time, captures from 2024–2025, non-detects recorded as numerical values below the LOD, and four records with very small recorded dry sample masses (0.18–0.42 g). Restriction checks kept captures within 80 km of the Fukushima Daiichi Nuclear Power Plant (index model), records that also had an index value (regional model) or records within the range of index values and capture dates of G3 (guild model). Species checks excluded raccoon dog, raccoon or the two control-captured species, or added origin (control capture versus rescue) as a covariate. Because origin was assigned by species, this covariate contrasts the two control-captured species (raccoon and masked palm civet) with all others. Specification checks added measurement year as a fixed effect, modelled year with a natural cubic spline, replaced the index by its rank or allowed a guild-specific residual SD. A further check treated spelling variants of the recorded Japanese names and names with a subspecies prefix as separate species. Clustering checks added a random intercept for municipality or for capture event, and bounding checks assigned 0.1 or 0.05 μSv/h to the 3 records with a censored index. Each estimate was compared with the main estimate by the sign of the posterior median and by whether its 95% CrI included zero.

Season and migration were examined in two further analyses. Season, represented by the sine and cosine of the day of the year of capture, was added to the species-adjusted index model and to the guild model. The guild model was also refitted without the 9 bird species coded as migratory in AVONET (migration score 3; Tobias et al., 2022; 26 records). These two analyses, the within- and between-species components (Section 2.6) and the class-only model (Section 2.7) are the four supplementary analyses.

2.9. Comparison with physical decay

For each posterior draw of the year coefficient, we computed its deviation from the physical-decay reference slope, $-\ln 2/T_{phys} = -0.0231$ year^{-1}, with $T_{phys} = 30.05 \pm 0.08$ years (Lavelle et al., 2018). This comparison was made between coefficients. Concentrations were not re-decay-corrected, and the deviation is not an ecological or biological half-life.

2.10. Computation and model checking

Models were fitted in R 4.6.0 (R Core Team, 2026) with brms 2.23.0 (Bürkner, 2017), which uses Stan (Carpenter et al., 2017) through rstan 2.32.7 (Stan Development Team, 2025). Continuous predictors were standardised within each model population, and coefficients were back-transformed to per-year and per-$\log_{10}$-unit scales. Convergence required R-hat ≤ 1.01, bulk and tail effective sample sizes ≥ 400, no divergent transitions, no iterations at the maximum tree depth and E-BFMI ≥ 0.3 for every chain. All models met these criteria except the capture-event models (Section 3.6). Prior predictive checks of the three main models showed that the priors were broad relative to the data. The central 95% of simulated concentrations spanned 5.2×10^{-11} to 1.1×10^{10} Bq/kg in the index model, with similar ranges in the other two models. Only 26%–27% of the simulated values lay within the range of the observed values and LODs (1.67–9,593 Bq/kg). Posterior predictive checks were run for the main, companion, guild and secondary models.

2.11. Posterior summaries

Estimates are reported as posterior medians with 95% CrIs, and species intercepts are summarised by posterior means. Ratios are exponentiated coefficients. The index effect is expressed as the fold difference per 10-fold higher index, and guild contrasts as ratios of adjusted concentrations. For the year coefficient, the posterior probability of a negative value is also reported.

3. Results

3.1. Study population and measurement structure

The master dataset contained 521 muscle sample records. After the 11 wild boar records were excluded (Section 2.1), 510 records remained, from animals captured between 2013 and 2025 (capture year missing for 28; Fig. 1a). Of these, 278 had detected Cs-137 concentrations, 99 were non-detects with a recorded LOD, 26 were non-detects without a usable LOD, 106 had no Cs-137 measurement and 1 carried a data-quality flag on its Cs-137 result (a suspected duplicate transcription). The flagged record entered no model (Fig. 1a). The index-model population (182 records) was concentrated in 2022–2024, with 129 records (70.9%). The years 2017–2021 contributed 50 records (27.5%), and 2025 contributed 3. Dried samples were measured 0.3–6.8 years after capture, generally sooner for later captures (storage effects are discussed in Section 4.2). The median dry-matter fraction by capture year ranged from 0.23 to 0.29 and was weakly related to storage time (Spearman correlation 0.11 with the time to measurement and 0.19 with the time to freeze-drying, in 148 records).

3.2. Fixed baseline environmental contamination

Muscle Cs-137 was positively associated with the index, conditional on year and species. In the species-adjusted index model, the index coefficient was 2.63 per $\log_{10}$ unit (95% CrI 2.17–3.10). A 10-fold higher index was therefore associated with a 13.8-fold higher concentration (95% CrI 8.80–22.1; Fig. 2a). On a log–log scale, this corresponds to an exponent of 1.14 (95% CrI 0.94–1.34), an interval that contains 1, the value

expected if concentrations were proportional to the index. Because the index includes natural radionuclides, the ratio refers to the air dose rate, not to Cs-137 deposition. The coefficient remained positive, with 95% CrIs excluding zero, in every converged sensitivity and guild model (Fig. 2a). With a municipality random intercept, the interval widened but the estimate changed little (ratio 13.7, 95% CrI 7.55–25.2). When the index was split into components, the within-species slope was 2.56 (95% CrI 2.09 to 3.03), close to the common slope, and the between-species slope was 3.81 (2.25 to 5.47). The companion model without the species term gave a larger coefficient (3.14, 95% CrI 2.63–3.66; open circle in Fig. 2a). In the species-adjusted regional model, concentrations were lower in Aizu (−2.18, 95% CrI −3.21 to −1.22) and higher in Hamadori (0.87, 0.34–1.39) than in Nakadori.

3.3. Temporal association

The direction of the temporal association depended on the model specification. The year coefficient was −0.088 (95% CrI −0.226 to 0.051) in the species-adjusted index model and 0.009 (−0.165 to 0.174) in the species-adjusted regional model (filled circles in Fig. 2b). The posterior probabilities of a negative coefficient were 0.89 and 0.46. In the guild model, the coefficient was −0.119 (−0.246 to 0.009), with a posterior probability of 0.97 of being negative. Companion models without the species term gave positive medians (index population: 0.113, 95% CrI −0.021 to 0.249; regional population: 0.252, 0.100–0.407; open circles in Fig. 2b). Across the sensitivity analyses of the species-adjusted models, 6 of 22 posterior medians had the opposite sign to the main-model median (triangles in Fig. 2b). The year coefficient (the effective temporal slope) was compared with the physical-decay reference slope (dashed line in Fig. 2b). Its deviation from that slope was −0.065 (95% CrI −0.203 to 0.074) in the index model and 0.032 (−0.142 to 0.197) in the regional model. These wide intervals do not distinguish physical decay from faster or slower change. When year was split into components, its effect was negative within species (−0.202, 95% CrI −0.351 to −0.055) and positive between species (0.280, 0.009 to 0.542). Species with later mean capture dates thus had higher adjusted concentrations, whereas within species, later captures had lower concentrations. Season terms changed the year coefficient little. Their sine coefficients were negative, which corresponds to higher concentrations in the second half of the year; the 95% CrI of the sine coefficient excluded zero in the guild model but not in the index model.

3.4. Between-species heterogeneity

The SD of the species random intercepts was 1.21 (95% CrI 0.80–1.79) in the species-adjusted index model. One SD therefore corresponds to a 3.35-fold difference in concentration. The SD was 1.40 (0.93–2.07) in the species-adjusted regional model. Posterior mean species intercepts in the index model spanned a 33.2-fold range of adjusted concentrations (lowest: grey heron, *Ardea cinerea*, 4 records; highest: Japanese giant flying squirrel, *Petaurista leucogenys*, 2 records). The 95% CrIs of 8 of the 38 species intercepts excluded zero. Compared with the companion models fitted to the same records, adding the species random intercept changed the posterior medians of the year coefficient by −0.203 (index model) and −0.246 (regional model) and the index coefficient by −0.506. The residual SD changed by −0.32 (index model) and −0.33 (regional

model). Fitting the companion models to these records instead of their own populations, which also include records without a unique species identification, changed their estimates little.

3.5. Guild contrasts

After adjustment for year, the index and species, the planned contrast G1 − G3, a comparison between mammals and birds, was 2.33 (95% CrI 1.57 to 3.15; ratio 10.3, 4.80–23.4). The other planned contrast, G5 − G3, was 0.44 (−0.33 to 1.24; Table 1; Fig. 3). G2 − G3 was 2.49 (1.45 to 3.59; ratio 12.1, 4.28–36.4). The four other contrasts between mammal and bird guilds were also positive, with 95% CrIs excluding zero. They include the contrasts against G4, the bird guild with the fewest left-censored records and hence the least dependent on censoring. Neither the two mammal guilds (G1 − G2: −0.14, −1.23 to 0.85; ratio 0.869, 0.291–2.34) nor the three bird guilds differed clearly from one another (Table 1). The residual group (American mink, 3 records), the only mammals with aquatic dependence, did not differ clearly from G1 (ratio 1.74, 0.313–8.43). G2 contained only 9 records of 4 species, and raccoon dog and raccoon contributed 62 of the 82 G1 records. Of the 33 G3 records, 20 were left-censored. Their LODs (median 2.36 Bq/kg) were not higher than those of all records (median 3.11 Bq/kg). The censoring therefore reflects low concentrations, not high LODs. The subset guild models gave similar contrasts, as did the guild model without the bird species coded as migratory and the guild model with season terms.

The species SD fell from 1.21 (0.80–1.79) without the guild term to 0.47 (0.18–0.86) with it, on the same 182 records, while the residual SD was essentially unchanged (1.09 and 1.07). A class-only model gave a similar species SD (0.47, 95% CrI 0.20 to 0.83) and a mammal − bird ratio of 8.70 (4.88–16.6). The two models had similar PSIS-LOO fits (elpd difference 1.2, SE 1.4, in favour of the class-only model). With a guild-specific residual SD, the contrasts were similar. The residual SD was larger in G4 than in G1, G3 and G5 and was uncertain in G2.

The index values and capture dates of G1 and G3 records overlapped only partly (Fig. 1c). Of the G1 records, 24 (29.3%) had index values above the G3 maximum of 1.0 μSv/h, and 36 (43.9%) were captured after the last G3 capture on 2 December 2023. Restricted to records within the G3 range of both (123 records, 31 species), G1 − G3 was 2.16 (1.40 to 3.07). G1 − G3 also remained positive, with 95% CrIs excluding zero, when raccoon dog, raccoon or the two control-captured species were excluded and when origin was added as a covariate (Fig. 3).

3.6. Sensitivity analyses and model checking

Sensitivity estimates are shown as triangles in Fig. 2. The index coefficient kept its sign, and its 95% CrI excluded zero, in every converged analysis. For the year coefficient, excluding 2024–2025 captures gave negative medians in both species-adjusted populations, whereas excluding numerical values below the LOD gave positive medians. All four of these 95% CrIs included zero. Including the record excluded for its LOD and assigning 0.1 or 0.05 μSv/h to the 3 censored-index records changed the estimates little. The capture-event random intercept could not be identified. In the index population, 170 of the 174 capture events

consisted of a single record, and the event SD could therefore not be separated from the residual SD. The capture-event models did not meet the convergence criteria, so these fits are not reported.

All other fitted models, including the five models of the four supplementary analyses, met the convergence criteria. In posterior predictive checks of the three main models, the observed statistics lay within the replicate 90% intervals with two exceptions. First, the number of detections among 2024 captures was lower than replicated in the index and guild models (36 of 43 observed; replicate 90% interval 37–41 in both models). Second, in the regional model, the 10th percentile of the ln detected values was lower than replicated. The shortfall of 2024 detections was concentrated in control-captured animals and also appeared in raccoon, G1 and Hamadori records, whereas rescued animals were within the interval. Of the 7 non-detects among 2024 captures, 4 came from one control capture in Namie on 2 May 2024 (three raccoons and one masked palm civet; index 5.20 μSv/h). Their dried samples weighed 0.18–0.42 g and had LODs of 65–185 Bq/kg wet weight. These are the four records with very small recorded dry sample masses (Section 2.8). Excluding them did not change the signs of the main estimates or whether their 95% CrIs included zero.

In the secondary models, the species SD of the detected-only concentration model, which spans both measurement periods, was 0.82 (0.55–1.20), compared with 1.21 (0.80–1.79) in the species-adjusted index model. The detection model of the index-model population gave a positive index coefficient, with a 95% CrI excluding zero. The measurement-period terms (fresh relative to dried samples) combine the change of measurement basis with any other difference between the periods. Their 95% CrIs included zero.

4. Discussion

Three findings stand out. First, muscle Cs-137 was associated with a contamination index fixed in 2012, and the association held within species. Second, pooled year estimates combined change within species with a shift in species composition towards mammals, and their direction was not robust across specifications. Third, most of the large differences among species lay between mammals and birds, and trait-based guilds added no detectable information beyond this difference between classes.

4.1. Fixed baseline environmental contamination

More than a decade after the accident, a contamination index fixed in 2012 remained informative about muscle Cs-137 in this sample of 38 species of wild mammals and birds. The direction agrees with positive associations between muscle Cs-137 and capture-site deposition in bear and wild boar in Fukushima (Nemoto et al., 2018). Such associations are not universal. They were weak in other wild boar surveys (Anderson et al., 2019) and were not detected within the Difficult-to-Return Zone, where contamination values spanned a narrow, high range (Saito et al., 2022a). Nor were they detected in great cormorants (*Phalacrocorax carbo*), a mobile aquatic-associated species (Saito et al., 2022b). Because species were captured at locations covering different index ranges (Fig. 1c), a common slope could mix differences within and between species. The within-species slope, however, was close to the common slope (Section 3.2). The

association is therefore present within species and is not only a product of where different species were captured.

Species-specific slopes were not fitted, and the models do not establish that the association has the same magnitude in every species, particularly in highly mobile aquatic-associated birds. The sensitivity and guild models reanalyse subsets of the same records with different specifications. Their agreement therefore shows stability under changes in model structure and population, not independent replication. The municipality random intercept widened the interval of the index coefficient by about a third while the estimate changed little. This indicates residual similarity among records from the same municipality that the main model does not represent.

The index represents the early contamination gradient, not contamination at capture, and several observations show why the two can differ. Deposition estimates from the third and fifth airborne surveys in 2011–2012 correlated closely, with ratios varying by land use (Kato et al., 2019). This correlation reflects agreement between early aerial surveys and does not show that spatial patterns remained stable through the 2017–2025 capture period. Air dose rates fell faster than expected from physical decay alone between the fourth and fifth surveys (MEXT, 2012), and decontamination reduced air dose rates on treated farmland by 20–70% (Onda et al., 2020). Airborne dose-rate maps tracked external doses of wild boar moderately well and outperformed single trap-site readings (Bontrager et al., 2024). That study, however, concerned external dose and more recent surveys, not internal Cs-137 concentrations. The index is therefore best interpreted as a measure of broad spatial differences in early contamination, which were associated with muscle Cs-137 in the sampled animals.

4.2. Temporal association

The pooled data did not identify the direction of the temporal association. Records were concentrated in 2022–2024 (Section 3.1), and capture year overlapped with several other factors. No G3 or G4 bird was captured after 13 December 2023, and only 3 of the 43 records from 2024 were birds. The 2024 records also included 26 of the 35 records with an index above 1.0 μSv/h and 26 of the 27 records counted for 3,600 s (Fig. 1c). The year estimate therefore depended on the adjustment used. Pooled year coefficients combine change within species with a shift in species composition (Section 4.3). Adding the guild term made the year coefficient more negative, probably because the guild term attributes the higher concentrations of the mammals to their guild and not to their later capture. Capture year also overlapped with measurement campaign and storage time. Adding measurement year as a fixed effect moved the year coefficient of the index model to −0.033.

The negative within-species year component (Section 3.3) may partly reflect storage. Within a measurement campaign, older captures had been stored longer (Section 3.1). If wet mass was weighed after frozen storage, water loss would have raised the converted wet-weight concentrations of older captures and thus produced an apparent decline within species. Even if the differences between capture years in the median dry-matter fraction (0.229–0.290) arose entirely from evaporation during storage, they would change converted

concentrations by at most 0.24 on the natural-log scale (about 27%). This is much less than the within-species change implied over the 7.8-year capture period (−0.202 per year, about −1.57 on the same scale). Differences between measurement campaigns in counting time, detectors or LOD definitions cannot be excluded. In addition, the within-species component is informed only by species with more than one record, and it does not establish a decline within species.

In other studies, temporal dynamics varied among species, sites and periods. In wild boar, monitoring from 2011 onwards showed declines in every region at region-specific rates, with a transient increase in Nakadori in fiscal year 2022 (Komatsu and Ikushima, 2026). Effective half-lives derived from transfer factors ranged from 1.2 years in green pheasant to 6.9 years in bear, while sika deer (*Cervus nippon*) and copper pheasant (*Syrmaticus soemmerringii*) showed no clear trend (Tagami et al., 2016). In a monkey population, concentrations decreased for several years and then showed no differences between 2017 and 2020 (Hayama et al., 2022), an interval that overlaps our capture window. These published half-lives are the source authors' metrics for single taxa, periods and models and are not equivalent to the multispecies annual coefficient estimated here. Reference ecological half-lives from single exponential fits are questionable where radionuclides are unevenly distributed and environmental redistribution dominates (Pröhl et al., 2006). In one long series from facility releases, decadal estimates of the ecological half-life varied widely (Gaines et al., 2021). The literature thus documents ecological variation between studies. The instability observed here, in contrast, is a sensitivity to model specification within one dataset.

4.3. Species composition and pooled estimates

Species differed widely, and the species composition of the sample shaped the pooled estimates. On the same records, adding a species random intercept changed the year coefficient by −0.203 (index model) and −0.246 (regional model) and the index coefficient by −0.506 (Section 3.4). The decompositions show how this happens. The index slope was 2.56 within species and 3.81 between species. Species from more contaminated locations, on average, thus had higher concentrations than the within-species slope alone would predict, and the coefficient of the model without the species term (3.14) lay between the two components. The year slope was −0.202 within species and +0.280 between species: species with later mean capture dates had higher concentrations, and later years had more mammal records (Section 4.2). The companion models without the species term accordingly gave positive year medians (Section 3.3). In both cases, omitting the species term moved the estimate towards the between-species value. These decompositions re-estimate the same records and are not independent tests. They show, nevertheless, that pooled temporal and environmental estimates from an opportunistic multispecies sample depend on which species were sampled, and where and when.

Published comparisons of species use different metrics: raw means of co-occurring mammals and birds (Watanabe et al., 2014), deposition-normalised transfer in game species (Tagami et al., 2016) and location-adjusted differences between wild boar and bear (Nemoto et al., 2018). Normalised concentrations also varied more than 100-fold among fungi and plants from one area, with species-specific temporal directions

(Komatsu et al., 2021). Our species SD is a different quantity: the spread of species intercepts after adjustment for year and baseline contamination. Large differences among species are not found in every study, however. Three game mammals in Poland showed no differences (Oloś and Dołhańczuk-Śródka, 2022), and in snakes, local contamination mattered more than species identity (Gerke et al., 2020).

4.4. Guild contrasts between and within classes

Because taxonomic class is one of the four traits, each guild lies within one class. Contrasts between mammal and bird guilds therefore compare classes as well as traits. The data resolved differences between classes but not between guilds within a class. The guild analysis is best read as a description of trait-based groups that largely coincide with taxonomic class and are dominated by a few species, not as a test of exposure pathways. Both mammal guilds had higher adjusted muscle Cs-137 than aquatic-associated birds (G3; Section 3.5). G1 was dominated by raccoon dog and raccoon and contained all 38 control-captured records. The G1 − G3 contrast nevertheless held when either species or the two control-captured species were excluded, and within the covariate range of G3.

The higher concentrations in mammals than in birds agree with observations from eastern Nihonmatsu (2011–2013), where several mammals exceeded birds and spot-billed duck had the lowest concentrations (Watanabe et al., 2014). That comparison, however, was small, descriptive and unadjusted. Differences in transfer between species also changed over time: mammals exceeded birds in 2011, but copper pheasant transfer approached that of mammals by 2015 (Tagami et al., 2016). In experimental trials, mallards (*Anas platyrhynchos*) eliminated radiocaesium rapidly after leaving contaminated ponds (Halford et al., 1983). This suggests that turnover and residence time offer an alternative to explanations based on feeding pathways. For the same reason, time spent in care before death, which was not recorded, may have lowered concentrations in rescued animals. If it differed between mammals and birds, it could account for part of the difference between classes.

Within mammals, the traits that distinguish the two mammal guilds (mainly diet, partly soil/litter contact) were not clearly associated with a difference in concentration (ratio 0.869, 95% CrI 0.291–2.34). G2 held only 9 records of 4 species, and its estimate is imprecise. The 3 American mink records, the only mammals with aquatic dependence, did not differ clearly from G1 (Section 3.5). Detrital and forest food-web pathways documented for invertebrates, amphibians and fish in single forests and catchments (Murakami et al., 2014; Sakai et al., 2016) provide ecological context but do not identify a mechanism for the vertebrates examined here.

Among birds, the guilds did not differ clearly. Aquatic-associated species do not universally have low concentrations. Great cormorants carried muscle Cs-137 similar to that of ducks and copper pheasant (Saito et al., 2022b). Among Canadian game birds exposed to low-level fallout, where most pooled samples were near background, piscivores and freshwater-feeding black ducks ranked among the higher groups (Stocki and Braune, 2020). Among passerines, species that nest and forage on the ground tended to be more likely to carry detectable Cs-137, but this association was marginal and concerned detection, not concentration

(Werner et al., 2025). Terrestrial birds also vary among themselves. Copper pheasant exceeded green pheasant in transfer (Tagami et al., 2016), and in a contaminated forest, one bird species carried about ten times more Cs-137 than others, without apparent links to foraging stratum (Murakami et al., 2015). Together with these studies, our results establish neither a general guild difference nor a causal ecological pathway, and they do not support a simple ranking of birds, whether of terrestrial above aquatic species or by trophic level.

Adding the guild term reduced the estimated between-species heterogeneity from 1.21 to 0.47 on the same records. A class-only model, however, reduced it to a similar value (0.47) and fitted similarly (Section 3.5). The reduction therefore reflects the mammal–bird difference. Elsewhere, too, trait scores did not absorb species heterogeneity: in a study of Cs-137 detection in passerines, species random effects remained substantial alongside a ground-use score (Werner et al., 2025). Although models predict that feeding category differentiates transfer more than class does (Whicker et al., 2023), our data cannot separate the two.

4.5. Limitations

The records derive from animals that were rescued after injury or disease or control-captured, and they do not form a probability sample of wildlife in Fukushima. Record numbers reflect neither population abundance nor sampling effort. In one study of white storks (*Ciconia ciconia*), wildlife rehabilitation admissions matched the wild population in mean pathogen prevalence but varied with bird origin, age and condition (Camacho et al., 2016). Admissions at a British rehabilitation centre were dominated by a few species (Mullineaux and Pawson, 2023). The direction of any sampling bias in Cs-137 in the present sample is unknown. Origin was assigned by species (Section 2.1), and excluding the two control-captured species did not change the main conclusions. The shortfall of 2024 detections was concentrated in control-captured animals, and 4 of the 7 non-detects among 2024 captures came from one control-capture event (Section 3.6). Species representation was uneven, and the guild comparisons carry the caveats described in Section 4.4.

Sex was recorded for 47 of the 182 records and age for 2. Neither was included in the analyses, and sex- and age-related variation therefore could not be evaluated. Muscle Cs-137 varies seasonally in some mammals (Nemoto et al., 2018). Season of capture entered only the supplementary models, which changed the main estimates little (Sections 3.3 and 3.5). An animal's capture location may not represent where it fed (Fukushima Prefecture, 2026), particularly for migratory waterfowl and seabirds in G3, such as swans and streaked shearwater (*Calonectris leucomelas*). The origin and precision of the capture coordinates were not documented, and errors in the assigned index could attenuate the estimated association. Home ranges, migratory movements, rescue-to-death intervals and any feeding during care were not recorded. In waterbirds on a contaminated reactor-cooling reservoir, residence time strongly shaped body burdens (Kennamer et al., 2017). Excluding the bird species coded as migratory changed the planned guild contrasts little (Section 3.5), but this global classification may not match each species' status in Japan, and the check is therefore coarse.

The environmental predictor derives from a single aerial survey in 2012, includes natural radionuclides and was affected by snow in parts of the surveyed area (Kato et al., 2019; MEXT, 2012). Records with a censored index were excluded, and assigning bounding values to them changed the estimates little. Whether a deposition-based index, such as the reconstructed fallout map of Kato et al. (2019), would show the same association was not examined.

In the concentration models, non-detects with a recorded LOD were modelled as left-censored values rather than substituted (Helsel, 2006). Most G3 records were censored, however, and the G3 reference level rests largely on censored observations. Detector models, calibration and the LOD calculation method were not stored with the records (Section 2.2). Because non-detects were censored at the reported LODs, any difference in LOD definition between measurement campaigns would carry into the censoring thresholds and hence into the G3 reference level and the year estimates. Recorded counting uncertainties (median 6.9% of the detected activity) were not propagated into the models. On the log scale, they are small relative to the residual SD. Records from the same capture event were treated as independent observations in the main models. Capture-event clustering could not be identified because almost every event comprised a single record, and clustering by municipality widened the interval of the index coefficient while changing its estimate little.

4.6. Implications and conclusions

In opportunistic records from rescue and wildlife-control programmes, which include non-game species, muscle Cs-137 remained associated with the 2012 contamination index once species differences were modelled, and the association held within species. Species identity mattered: one SD of species intercepts corresponded to a 3.35-fold difference, and most of this heterogeneity lay between mammals and birds. Omitting species random intercepts raised the year and index coefficients, because pooled estimates also reflected differences between species. Pooled year estimates thus combined a negative within-species component with a shift towards mammals in later years. The direction of temporal estimates depended on model specification in a sample concentrated in 2022–2024, and the main year coefficients could not be distinguished from the physical-decay reference. Mammal guilds had higher concentrations than bird guilds, a difference that may also reflect unrecorded time in care and foraging range. A class-only model fitted about as well as the guild model, and guilds defined from species traits did not differ clearly within a class. Opportunistic multispecies radiocaesium data from wildlife should therefore be analysed with species-level effects. A trait grouping that includes taxonomic class should be compared with a class-only model before it is interpreted as reflecting exposure pathways. For monitoring, temporal change in multispecies data should be estimated within species or with species composition included in the model. Records should also document each animal's origin, the time it spent in care and the measurement conditions.

Acknowledgements

We thank all those who assisted with the collection, recording, sample processing and measurement of the wild animals.

Funding

Hisashi Komatsu received funding from the Environmental Radioactivity Research Network Center (ERAN) (Grant No. P25-34). The funder had no role in study design, data collection and analysis, decision to publish, or preparation of the manuscript.

Declaration of competing interest

The authors declare that they have no known competing financial interests or personal relationships that could have appeared to influence the work reported in this paper.

Data availability

The source data are held by the Fukushima Prefectural Centre for Environmental Creation. Availability of the underlying data is subject to the Centre's data-management and disclosure procedures.

References

Anderson, D., Okuda, K., Hess, A., Nanba, K., Johnson, T., Takase, T., Hinton, T., 2019. A comparison of methods to derive aggregated transfer factors using wild boar data from the Fukushima Prefecture. Journal of Environmental Radioactivity 197, 101–108. https://doi.org/10.1016/j.jenvrad.2018.12.009.

Beresford, N.A., Yankovich, T.L., Wood, M.D., Fesenko, S., Andersson, P., Muikku, M., Willey, N.J., 2013. A new approach to predicting environmental transfer of radionuclides to wildlife: a demonstration for freshwater fish and caesium. Science of The Total Environment 463–464, 284–292. https://doi.org/10.1016/j.scitotenv.2013.06.013.

Bontrager, H.L., Hinton, T.G., Okuda, K., Beasley, J.C., 2024. The impact of sampling scale: A comparison of methods for estimating external contaminant exposure in free-ranging wildlife. Science of The Total Environment 921, 171012. https://doi.org/10.1016/j.scitotenv.2024.171012.

Bürkner, P.C., 2017. brms: An R Package for Bayesian Multilevel Models Using Stan. Journal of Statistical Software 80(1). https://doi.org/10.18637/jss.v080.i01.

Camacho, M., Hernández, J.M., Lima-Barbero, J.F., Höfle, U., 2016. Use of wildlife rehabilitation centres in pathogen surveillance: A case study in white storks (Ciconia ciconia). Preventive Veterinary Medicine 130, 106–111. https://doi.org/10.1016/j.prevetmed.2016.06.012.

Carpenter, B., Gelman, A., Hoffman, M.D., Lee, D., Goodrich, B., Betancourt, M., Brubaker, M., Guo, J., Li, P., Riddell, A., 2017. Stan: A Probabilistic Programming Language. Journal of Statistical Software 76(1). https://doi.org/10.18637/jss.v076.i01.

Fukushima Prefecture, 2026. 野生鳥獣の放射線モニタリング調査結果 [Results of radiation monitoring of wild birds and mammals]. Fukushima Prefecture website, Fukushima reconstruction information portal (page updated 27 April 2026). In Japanese. https://www.pref.fukushima.lg.jp/site/portal/wildlife-radiationmonitoring1.html (accessed 27 September 2026).

Gaines, K.F., Novak, P.M., Novak, J.M., 2021. Ecological half-life of radiocesium in white-tailed deer on the Department of Energy's Savannah River Site: What can a half century of field monitoring tell us? Journal of Environmental Radioactivity 235–236, 106654. https://doi.org/10.1016/j.jenvrad.2021.106654.

GBIF Secretariat, 2023. GBIF Backbone Taxonomy. Checklist dataset. https://doi.org/10.15468/39omei (accessed via the GBIF species match API on 25 September 2026).

Gerke, H.C., Hinton, T.G., Takase, T., Anderson, D., Nanba, K., Beasley, J.C., 2020. Radiocesium concentrations and GPS-coupled dosimetry in Fukushima snakes. Science of The Total Environment 734, 139389. https://doi.org/10.1016/j.scitotenv.2020.139389.

Halford, D.K., Markham, D.O., White, G.C., 1983. Biological elimination rates of radioisotopes by mallards contaminated at a liquid radioactive waste disposal area. Health Physics 45(3), 745–756. https://doi.org/10.1097/00004032-198309000-00016.

Hayama, S.I., Nakiri, S., Nakanishi, S., Ishii, N., Uno, T., Kato, T., Konno, F., Kawamoto, Y., Tsuchida, S., Ochiai, K., Omi, T., 2013. Concentration of radiocesium in the wild Japanese monkey (Macaca fuscata) over the first 15 months after the Fukushima Daiichi nuclear disaster. PLoS ONE 8(7), e68530. https://doi.org/10.1371/journal.pone.0068530.

Hayama, S.I., Tanaka, A., Nakanishi, S., Konno, F., Kawamoto, Y., Ochiai, K., Omi, T., 2022. Time dependence of ^{137}Cs contamination in wild Japanese monkeys after the Fukushima Daiichi nuclear accident. Environmental Science and Pollution Research 29(58), 88359–88368. https://doi.org/10.1007/s11356-022-23707-0.

Helsel, D.R., 2006. Fabricating data: how substituting values for nondetects can ruin results, and what can be done about it. Chemosphere 65(11), 2434–2439. https://doi.org/10.1016/j.chemosphere.2006.04.051.

Kato, H., Onda, Y., Gao, X., Sanada, Y., Saito, K., 2019. Reconstruction of a Fukushima accident-derived radiocesium fallout map for environmental transfer studies. Journal of Environmental Radioactivity 210, 105996. https://doi.org/10.1016/j.jenvrad.2019.105996.

Kennamer, R.A., Oldenkamp, R.E., Leaphart, J.C., King, J.D., Bryan, A.L., Beasley, J.C., 2017. Radiocesium in migratory aquatic game birds using contaminated U.S. Department of Energy reactor-cooling reservoirs: A long-term perspective. Journal of Environmental Radioactivity 171, 189–199. https://doi.org/10.1016/j.jenvrad.2017.02.022.

Komatsu, H., Ikushima, S., 2026. Factors affecting log-transformed muscle ^{137}Cs concentrations in wild boars in Fukushima Prefecture over 14 years. PLOS One 21(3), e0344189. https://doi.org/10.1371/journal.pone.0344189.

Komatsu, M., Hashimoto, S., Matsuura, T., 2021. Effects of species and geo-information on the ^{137}Cs concentrations in edible wild mushrooms and plants collected by residents after the Fukushima nuclear accident. Scientific Reports 11(1), 22470. https://doi.org/10.1038/s41598-021-01816-z.

Lavelle, K.B., Essex, R.M., Carney, K.P., Cessna, J.T., Hexel, C.R., 2018. A reference material for evaluation of ^{137}Cs radiochronometric measurements. Journal of Radioanalytical and Nuclear Chemistry 318(1), 195–208. https://doi.org/10.1007/s10967-018-6061-4.

MEXT (Ministry of Education, Culture, Sports, Science and Technology, Japan), 2012. Results of the (i) Fifth Airborne Monitoring Survey and (ii) Airborne Monitoring Survey Outside 80km from the Fukushima Dai-ichi NPP (released 28 September 2012). MEXT press release (English version), 20 pp. Archived on the RAMDAS website of the Nuclear Regulation Authority, Japan. https://radioactivity.nra.go.jp/cont/en/results/land/airborne/survey-results/203_0928_14e.pdf.

Ministry of the Environment, Japan, 2026. きのこ類、山菜、野生鳥獣肉の検査結果の推移 [Trends in inspection results of mushrooms, wild vegetables and wild game meat]. In: 放射線による健康影響等に関する統一的な基礎資料（令和 7 年度版） [Unified basic data on health effects of radiation, FY2025 edition], Chapter 8, Section 8.5 (page revised 31 March 2026). In Japanese. https://www.env.go.jp/chemi/rhm/current/08-05-03.html (accessed 27 September 2026).

Mullineaux, E., Pawson, C., 2023. Trends in Admissions and Outcomes at a British Wildlife Rehabilitation Centre over a Ten-Year Period (2012–2022). Animals 14(1), 86. https://doi.org/10.3390/ani14010086.

Murakami, M., Ohte, N., Suzuki, T., Ishii, N., Igarashi, Y., Tanoi, K., 2014. Biological proliferation of cesium-137 through the detrital food chain in a forest ecosystem in Japan. Scientific Reports 4(1), 3599. https://doi.org/10.1038/srep03599.

Murakami, M., Suzuki, T., Ohte, N., Ishii, N., 2015. 森林生態系における放射性セシウムの鳥類への移行 [Biological proliferation of ^{137}Cs to forest bird species in a forest ecosystem]. Japanese Journal of Ornithology 64(1), 55–61. In Japanese with English abstract. https://doi.org/10.3838/jjo.64.55.

Nemoto, Y., Saito, R., Oomachi, H., 2018. Seasonal variation of Cesium-137 concentration in Asian black bear (Ursus thibetanus) and wild boar (Sus scrofa) in Fukushima Prefecture, Japan. PLOS ONE 13(7), e0200797. https://doi.org/10.1371/journal.pone.0200797.

Oloś, G., Dołhańczuk-Śródka, A., 2022. Effective and environmental half-lives of radiocesium in game from Poland. Journal of Environmental Radioactivity 248, 106870. https://doi.org/10.1016/j.jenvrad.2022.106870.

Onda, Y., Taniguchi, K., Yoshimura, K., Kato, H., Takahashi, J., Wakiyama, Y., Coppin, F., Smith, H., 2020. Radionuclides from the Fukushima Daiichi Nuclear Power Plant in terrestrial systems. Nature Reviews Earth & Environment 1(12), 644–660. https://doi.org/10.1038/s43017-020-0099-x.

Ornithological Society of Japan, 2024. Check-list of Japanese Birds, 8th Revised Edition. Ornithological Society of Japan (list version 2024-10-08; errata of 2025-06-09). https://ornithology.jp/checklist.html.

Pröhl, G., Ehlken, S., Fiedler, I., Kirchner, G., Klemt, E., Zibold, G., 2006. Ecological half-lives of ^{90}Sr and ^{137}Cs in terrestrial and aquatic ecosystems. Journal of Environmental Radioactivity 91(1–2), 41–72. https://doi.org/10.1016/j.jenvrad.2006.08.004.

R Core Team, 2026. R: A Language and Environment for Statistical Computing. R Foundation for Statistical Computing, Vienna, Austria. https://doi.org/10.32614/R.manuals.

Saito, R., Kabeya, M., Nemoto, Y., Oomachi, H., 2019. Monitoring ^{137}Cs concentrations in bird species occupying different ecological niches; game birds and raptors in Fukushima Prefecture. Journal of Environmental Radioactivity 197, 67–73. https://doi.org/10.1016/j.jenvrad.2018.10.016.

Saito, R., Kumada, R., Inami, K., Kanda, K., Kabeya, M., Tamaoki, M., Nemoto, Y., 2022a. Monitoring of radioactive cesium in wild boars captured inside the difficult-to-return zone in Fukushima Prefecture over a 5-year period. Scientific Reports 12(1), 5667. https://doi.org/10.1038/s41598-022-08444-1.

Saito, R., Nemoto, Y., Kumada, R., Kabeya, M., Funaki, Y., Kanda, K., Jo, J., 2022b. 福島県内のカワウ（Phalacrocorax carbo）の体内に含まれる放射性セシウム濃度のモニタリング調査 [Monitoring results of radiocaesium contamination in great cormorants (Phalacrocorax carbo) in Fukushima Prefecture]. Journal of the Society for Remediation of Radioactive Contamination in the Environment 10(4), 157–164. In Japanese. https://doi.org/10.82733/jsrrce.10.4_157.

Sakai, M., Gomi, T., Negishi, J.N., Iwamoto, A., Okada, K., 2016. Different cesium-137 transfers to forest and stream ecosystems. Environmental Pollution 209, 46–52. https://doi.org/10.1016/j.envpol.2015.11.025.

Stan Development Team, 2025. RStan: the R interface to Stan. R package version 2.32.7. https://mc-stan.org/.

Stocki, T.J., Braune, B.M., 2020. Radiocesium in Canadian game Birds Harvested during 1989-95. Journal of Environmental Radioactivity 225, 106337. https://doi.org/10.1016/j.jenvrad.2020.106337.

Tagami, K., Howard, B.J., Uchida, S., 2016. The Time-Dependent Transfer Factor of Radiocesium from Soil to Game Animals in Japan after the Fukushima Dai-ichi Nuclear Accident. Environmental Science & Technology 50(17), 9424–9431. https://doi.org/10.1021/acs.est.6b03011.

Tobias, J.A., Sheard, C., Pigot, A.L., Devenish, A.J.M., Yang, J., Sayol, F., et al., 2022. AVONET: morphological, ecological and geographical data for all birds. Ecology Letters 25(3), 581–597. https://doi.org/10.1111/ele.13898.

UNSCEAR (United Nations Scientific Committee on the Effects of Atomic Radiation), 2022. UNSCEAR 2020/2021 Report, Volume II, Scientific Annex B: Levels and effects of radiation exposure due to the accident at the Fukushima Daiichi Nuclear Power Station: implications of information published since the UNSCEAR 2013 Report. United Nations, New York (Sales No. E.22.IX.2; ISBN 978-92-1-139207-4); with the corrigendum of September 2023. https://doi.org/10.18356/9789210010047.

Watanabe, I., Nomura, A., Masukawa, T., Ozaki, H., Watai, C., Hayashidani, H., Gomi, T., Yoshida, M., Yokoyama, T., 2014. 福島県二本松市東部で採取された野生動物(数種の鳥類および哺乳類)の放射性セシウム蓄積 [Radioactive Cs accumulations in wildlife (some species of birds and mammals) collected from eastern part of Nihonmatsu City, Fukushima Prefecture, Japan]. Journal of the Society for Remediation of Radioactive Contamination in the Environment 2(4), 241–250. In Japanese. https://doi.org/10.82733/jsrrce.2.4_241.

Werner, C.S., Chapman, M., Rhodes, O.E., DeVault, T.L., 2025. Uptake of metals, metalloids, and radiocesium varies with habitat use among passerine communities at coal combustion and nuclear fission legacy waste sites. Environmental Pollution 367, 125608. https://doi.org/10.1016/j.envpol.2024.125608.

Whicker, J.J., Gerard, J.L., Inglis, J.D., Conrad, C., 2023. Allometric-kinetic model predictions of concentration ratios for anthropogenic radionuclides across animal classes and food selection. Journal of Environmental Radioactivity 270, 107312. https://doi.org/10.1016/j.jenvrad.2023.107312.

Wilman, H., Belmaker, J., Simpson, J., de la Rosa, C., Rivadeneira, M.M., Jetz, W., 2014. EltonTraits 1.0: species-level foraging attributes of the world's birds and mammals. Ecology 95(7), 2027. https://doi.org/10.1890/13-1917.1.

Tables

Table 1. Guild contrasts of the guild model (182 records, 38 species), adjusted for year, the fixed baseline environmental contamination index and species (random intercept). Posterior medians with 95% credible intervals (CrIs); ln, difference on the natural-log scale; ratio, exponentiated difference. G3 is the reference category. Records (species) per guild: G1 82 (6), G2 9 (4), G3 33 (11), G4 24 (5), G5 31 (11).

Contrast	ln difference (95% CrI)	Ratio (95% CrI)
G1 − G3, planned (soil/litter-associated terrestrial mammals vs aquatic-associated birds)	2.33 (1.57 to 3.15)	10.3 (4.80–23.4)
G2 − G3 (herbivorous mammals with low or medium soil/litter contact vs aquatic-associated birds)	2.49 (1.45 to 3.59)	12.1 (4.28–36.4)
G1 − G2 (within mammals)	−0.14 (−1.23 to 0.85)	0.869 (0.291–2.34)
G5 − G3, planned (other terrestrial birds vs aquatic-associated birds)	0.44 (−0.33 to 1.24)	1.56 (0.716–3.47)
G4 − G3 (terrestrial vertebrate-eating birds vs aquatic-associated birds)	0.65 (−0.22 to 1.50)	1.91 (0.799–4.48)
G4 − G5 (within terrestrial birds)	0.21 (−0.69 to 1.08)	1.23 (0.502–2.94)

Figure captions

Fig. 1. Coverage of the muscle Cs-137 records. (a) Muscle sample records by capture year and Cs-137 measurement status (510 records after the exclusion of wild boar; 28 without a recorded capture year, shown as n/a); brackets mark the capture years of records measured as fresh (2013–2017) and as dried (2017–2025) samples. (b) Records per species in the index-model population (182 records, 38 species), grouped by guild. (c) Fixed baseline environmental contamination index (air dose rate from the fifth airborne monitoring survey at the capture location; log scale) against capture date for the same records (symbol shape and colour by guild); filled symbols, Cs-137 detected; open symbols, non-detects (left-censored). Dashed lines mark the maximum index (1.0 μSv/h) and the last capture date (2 December 2023) of G3 records. G1, soil/litter-associated terrestrial mammals; G2, herbivorous mammals with low or medium soil/litter contact; G3, aquatic-associated birds; G4, terrestrial vertebrate-eating birds; G5, other terrestrial birds; residual, mammals using aquatic food.

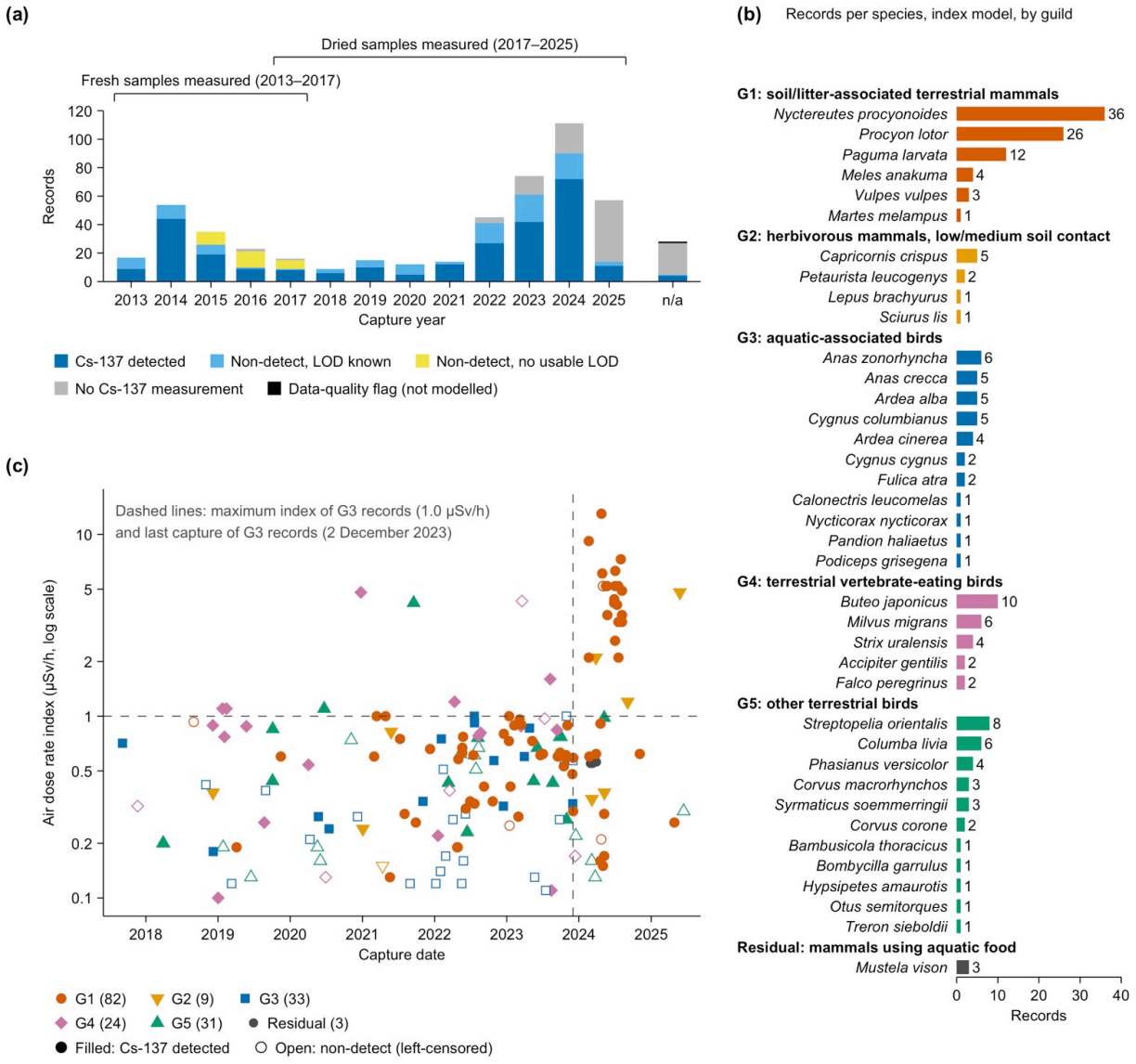


Fig. 2. Coefficients of (a) the fixed baseline environmental contamination index (per $\log_{10}$ unit of the air dose rate at the capture location) and (b) year across model specifications, on the natural-log (ln) scale of wet-weight muscle Cs-137. Points are posterior medians and horizontal lines 95% credible intervals (CrIs); the top axes express the same coefficients as the fold difference per 10-fold higher index (a) and as the percentage change per year (b). Filled circles, the species-adjusted index and regional models; open circles, companion models without the species term; filled squares, the guild model and its variant with a guild-specific residual SD; triangles, sensitivity analyses (Section 2.8). The dashed line in (b) is the physical-decay reference slope of Cs-137 (−0.0231 per year). The regional models adjust for region instead of the index and have no index coefficient; the natural-spline variant was compared only for the year coefficient, the variant restricted to captures within 80 km of FDNPP only for the index coefficient, and the rank-transformed index variant (on a different scale) is not shown. The capture-event models, which did not meet the convergence criteria (Section 3.6), are not shown. FDNPP, Fukushima Daiichi Nuclear Power Plant.

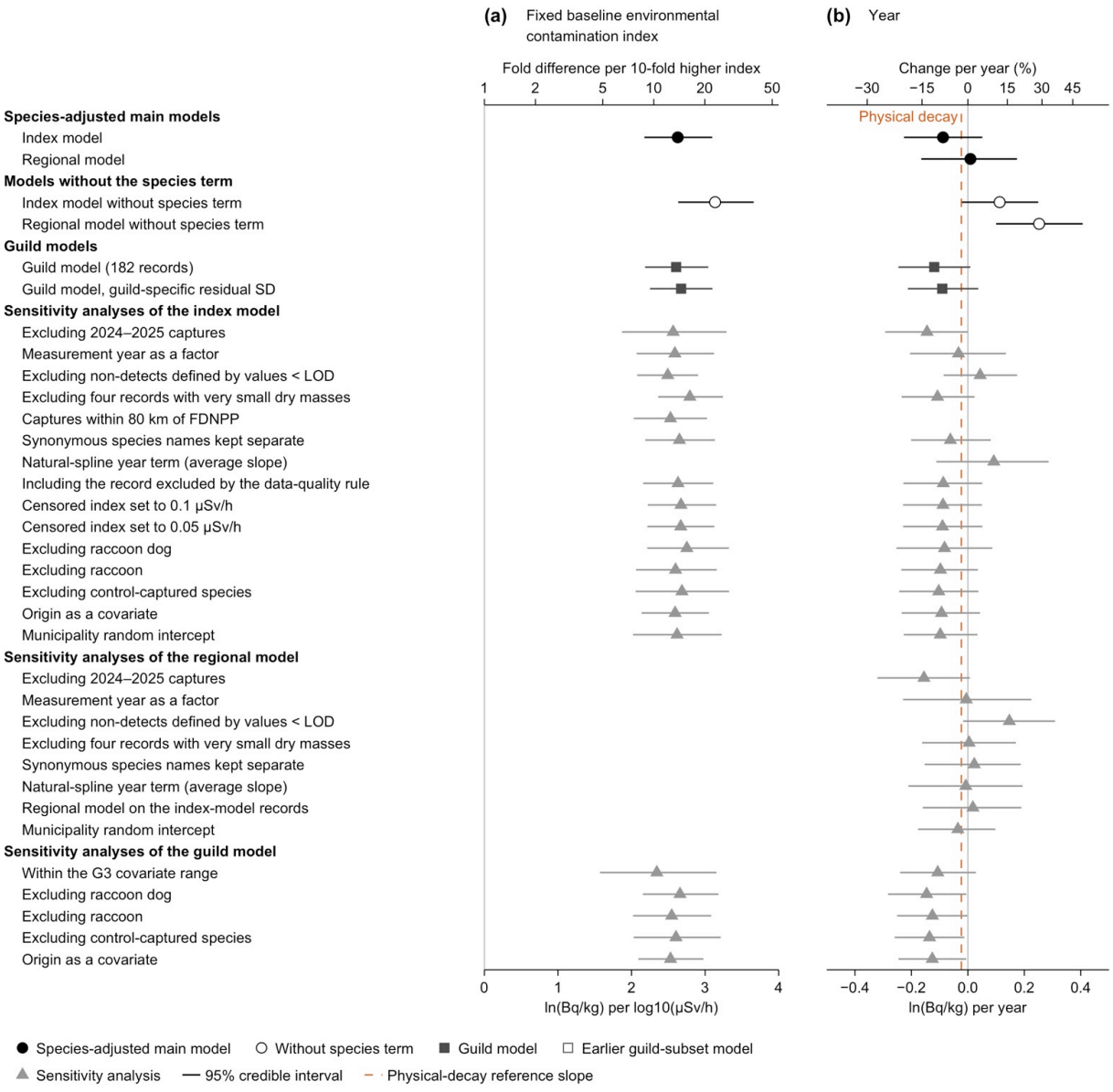
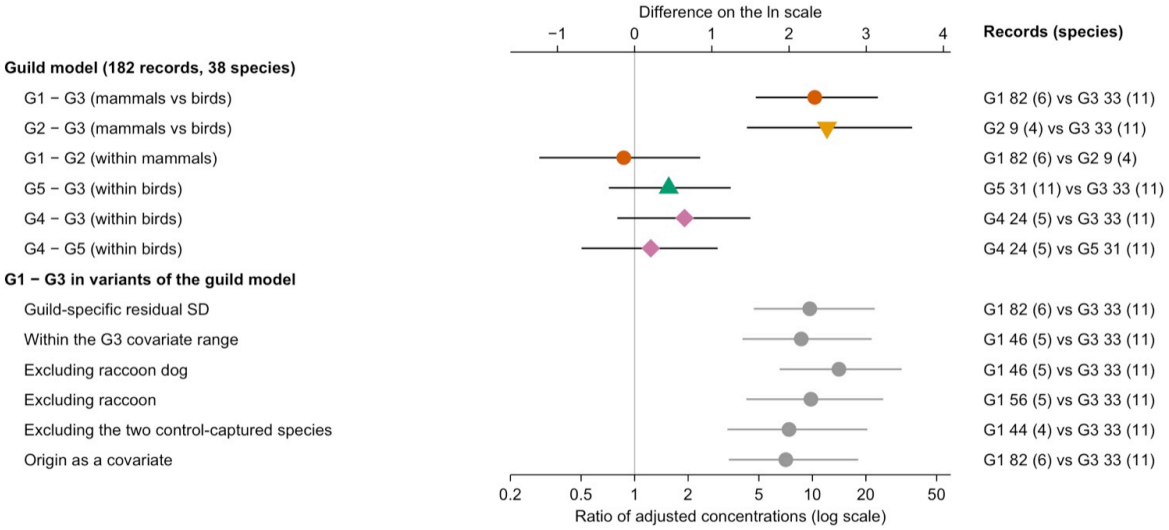


Fig. 3. Guild contrasts of the guild model (182 records, 38 species) as ratios of adjusted concentrations (log scale; the top axis gives the same contrast on the ln scale). Points are posterior medians and horizontal lines 95% CrIs. Upper block: the six contrasts of the guild model (G1 − G3 and G5 − G3 planned, the others exploratory); lower block: G1 − G3 in the variant with a guild-specific residual SD and in the sensitivity analyses of the guild model (Section 2.8). G1, soil/litter-associated terrestrial mammals; G2, herbivorous mammals with low or medium soil/litter contact; G3, aquatic-associated birds; G4, terrestrial vertebrate-eating birds; G5, other terrestrial birds. Right-hand column: records (species) of the two groups compared.



G1, soil/litter-associated terrestrial mammals; G2, herbivorous mammals with low or medium soil/litter contact; G3, aquatic-associated birds; G4, terrestrial vertebrate-eating birds; G5, other terrestrial birds.